SAND2018-3648C

A-Φ Formulation Time Domain Integral Equations Free from Interior Resonances

T. E. Roth[1,2] **and W. C. Chew**[2,3]

[1]Sandia National Laboratories, Albuquerque, New Mexico, USA
[2]Department of Electrical and Computer Engineering, University of Illinois at Urbana-Champaign, Urbana, Illinois, USA
[3]Department of Electrical and Computer Engineering, Purdue University, West Lafayette, Indiana, USA

Abstract— The **A**-Φ formulation has been proposed as a new paradigm for deriving computational electromagnetics methods that do not suffer from the various manifestations of low frequency breakdown that have plagued traditional approaches. This formulation utilizes equations developed in terms of the magnetic vector potential (**A**) and electric scalar potential (Φ), which allows them to overcome many of the limitations inherent to methods based directly on the electric and magnetic fields. The predominant limitation overcome by the **A**-Φ formulation is the aforementioned low frequency breakdown inherent in traditional approaches. Additionally, the **A**-Φ formulation also produces systems which can be effectively and efficiently preconditioned in a simpler manner than those based directly on electric and magnetic field. This formulation is also better suited for integration with quantum physics applications where description of electromagnetic effects is more naturally represented with **A** and Φ. Recent work has developed **A**-Φ formulation time domain integral equations (TDIEs) which were stable over a wide range of problems and could maintain accuracy to very low frequencies. However, these equations were susceptible to being corrupted by interior resonances. The presence of interior resonances lowered the accuracy of the method when extracting frequency domain results near the resonances and also led to the eventual instability of the numerical method if too many interior resonances were excited (exactly synonymous to how the EFIE or MFIE would behave). This precluded the original **A**-Φ formulation TDIEs from being used to analyze multiscale structures that had closed regions approximately a few wavelengths or larger in size. This work proposes a modification to the initial **A**-Φ formulation TDIEs that makes them immune to issues related to interior resonances. This allows the new set of equations proposed in this work to be applied to deeply multiscale problems previously unable to be analyzed with this formulation. Numerical results are used to demonstrate that this new method is free from interior resonances. Further, it is shown that the other favorable qualities of this system are not lost due to the modifications proposed in this work.

1. INTRODUCTION

Past implementations of **A**-Φ surface integral equations (SIE) in the time domain were susceptible to interior resonances [1]. This rendered them unsuitable for analysis of multiscale geometries that may contain closed surfaces that are comparable in size to the wavelengths contained within the exciting pulse. This work presents a new **A**-Φ SIE that is free from interior resonances, allowing it to be used for the analysis of structures over very broad ranges of frequency.

The methodology adopted for deriving a new set of **A**-Φ equations with the desired properties follows the general approach laid out in [1]. First, one finds a set of **E**-**H** integral equations with the desired properties and then converts these equations into their equivalent **A**-Φ representation. Throughout this process, the relevant Sobolev spaces that act as the domain and range of the integral operators are monitored. This determines a set of equations that can be stably discretized, as well as suggests which basis and testing functions should be utilized in the discretization process. Note that for brevity, the details of the Sobolev space analysis for these equations are not discussed here. However, this analysis is available for the original **A**-Φ TDIEs in [2].

The remainder of this work is organized into the following sections. Section 2 presents the derivation and discretization of a new set of **A**-Φ time domain integral equations (TDIEs) that are free from interior resonances. Following this, Section 3 demonstrates the qualities of these new TDIEs through appropriate numerical examples. Finally, Section 4 discusses conclusions and future work related to **A**-Φ TDIEs.

2. FORMULATION

Past **A**-Φ TDIEs began from the EFIE for a scattering surface defined by S, which is

$$\int_S \left[\mu \frac{\dot{\mathbf{J}}(\mathbf{r}',\tau)}{4\pi R} + \nabla \frac{\rho(\mathbf{r}',\tau)}{4\pi R\epsilon}\right] dS' = \mathbf{E}^{\text{inc}}(\mathbf{r},t). \tag{1}$$

In (1), $\tau = t - R/c$ is the retarded time, the current density is $\mathbf{J}$, the charge density is ρ, the incident electric field is $\mathbf{E}^{\text{inc}}$, and a dot over a function denotes a time derivative. As initial conditions, it is assumed that the incident field on S is zero for all $t \leq 0$.

From the EFIE, two sets of **A**-Φ TDIEs were derived in [1]. The first set, termed the differentiated **A**-Φ integral equations (D-APIE) is

$$\int_S \left[\mu \frac{\dot{\mathbf{J}}(\mathbf{r}',\tau)}{4\pi R} - \nabla \frac{\Pi(\mathbf{r}',\tau)}{4\pi R}\right] dS' = -\dot{\mathbf{A}}^{\text{inc}}(\mathbf{r},t) \tag{2}$$

$$\int_S \left[\frac{\nabla' \cdot \mathbf{J}(\mathbf{r}',\tau)}{4\pi R\epsilon} - \frac{\dot{\Pi}(\mathbf{r}',\tau)}{4\pi R}\right] dS' = \dot{\Phi}^{\text{inc}}(\mathbf{r},t), \tag{3}$$

where the name comes from the fact that these equations have temporally differentiated excitations. In (2) and (3), $\Pi = \hat{n}' \cdot \dot{\mathbf{A}}$, which along with $\mathbf{J}$ are the unknowns for this system. The physical meaning of Π can be understood by noting that it is a component of the charge density. The second set of equations, termed the APIE, is

$$\int_S \left[\mu \frac{\mathbf{J}(\mathbf{r}',\tau)}{4\pi R} - \nabla \int_{-\infty}^{\tau} \frac{\Pi(\mathbf{r}',t')}{4\pi R} dt'\right] dS' = -\mathbf{A}^{\text{inc}}(\mathbf{r},t) \tag{4}$$

$$\int_S \left[\int_{-\infty}^{\tau} \frac{\nabla' \cdot \mathbf{J}(\mathbf{r}',t')}{4\pi R\epsilon} dt' - \frac{\Pi(\mathbf{r}',\tau)}{4\pi R}\right] dS' = \Phi^{\text{inc}}(\mathbf{r},t). \tag{5}$$

Both of these sets of equations have been shown to be able to be stably discretized, as well as able to maintain accuracy and stability at very low frequencies where the EFIE becomes unstable [1].

Although the D-APIE and APIE have shown improvement over the EFIE for analyzing multiscale structures, they cannot be applied to systems that are deeply multiscale. The issue is that, like the EFIE, these equations are susceptible to interior resonances. In the time domain, this can affect the solution by lowering the accuracy if only a very small number of resonances of the structure are contained within the exciting pulse. At higher frequencies, when many interior resonances can be excited, the time marching process becomes unstable making the simulation completely unusable.

The typical remedy for interior resonances is to instead solve the CFIE when using the **E**-**H** formulation [3]. Using this as inspiration for the **A**-Φ formulation, it is expected that APIEs derived from the CFIE as a starting point will also be free from interior resonances, while still maintaining their favorable low frequency properties. This theory is tested in this work by deriving and implementing a new D-APIE.

2.1. Derivation

Through past work, the EFIE has already been converted into the **A**-Φ formulation in such a way that it can be stably discretized, represented by (2) and (3). As a result, to convert the CFIE into the **A**-Φ formulation, all that remains is to convert the MFIE.

To begin this process we take the time domain MFIE, which is

$$\frac{1}{2}\mathbf{J}(\mathbf{r},t) - \hat{n} \times \text{P.V.} \int_S \left[\frac{\dot{\mathbf{J}}(\mathbf{r}',\tau)}{4\pi R^2 c} + \frac{\mathbf{J}(\mathbf{r}',\tau)}{4\pi R^3}\right] \times \boldsymbol{R}\, dS' = \hat{n} \times \mathbf{H}^{\text{inc}}(\mathbf{r},t). \tag{6}$$

Since $\mathbf{J}$ is one of the unknowns already accounted for in the D-APIE, it does not need to be modified to convert it to the **A**-Φ formulation. This leaves only the excitation to be rewritten, which can be easily done to give

$$\frac{1}{2}\mu\mathbf{J}(\mathbf{r},t) - \hat{n} \times \text{P.V.} \int_S \left[\mu\frac{\dot{\mathbf{J}}(\mathbf{r}',\tau)}{4\pi R^2 c} + \mu\frac{\mathbf{J}(\mathbf{r}',\tau)}{4\pi R^3}\right] \times \boldsymbol{R}\, dS' = \hat{n} \times \nabla \times \mathbf{A}^{\text{inc}}(\mathbf{r},t). \tag{7}$$

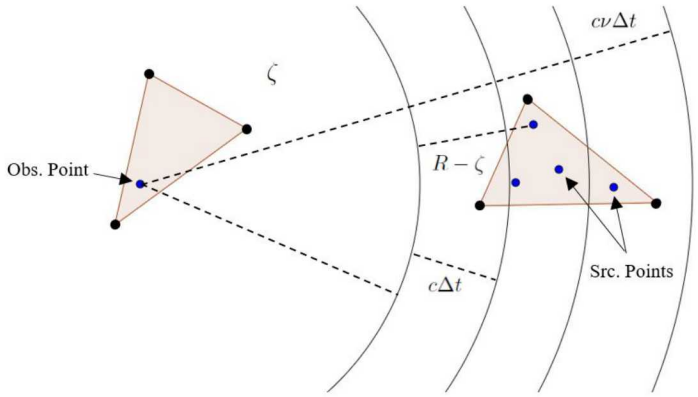

Figure 1: Geometry defining the various parameters used in the separable expansion of the Green's function.

Before adding (7) into the system defined by (2) and (3), it is important to determine if the temporal order of the Sobolev spaces acting as the domain and range of the integral operators in (7) are commensurate with those of (2) and (3). This is necessary to ensure that the system can be consistently discretized, producing stable results in practice [2]. Fortunately, the temporal Sobolev spaces are the same, so no further modifications are needed [4]. This allows (7) to be added to the D-APIE system given in (2) and (3) without damaging the stability properties of this system. Further, this modification yields a new system free from interior resonances. This system is

$$\frac{1}{2}\mu\mathbf{J}(\mathbf{r},t)-\hat{n}\times\text{P.V.}\int_S\left[\mu\frac{\dot{\mathbf{J}}(\mathbf{r}',\tau)}{4\pi R^2 c}+\mu\frac{\mathbf{J}(\mathbf{r}',\tau)}{4\pi R^3}\right]\times\boldsymbol{R}\,dS'+\int_S\left[\mu\frac{\dot{\mathbf{J}}(\mathbf{r}',\tau)}{4\pi R}-\nabla\frac{\Pi(\mathbf{r}',\tau)}{4\pi R}\right]dS' = -\dot{\mathbf{A}}^{\text{inc}}(\mathbf{r},t)+\hat{n}\times\nabla\times\mathbf{A}^{\text{inc}}(\mathbf{r},t) \quad (8)$$

$$\int_S\left[\frac{\nabla'\cdot\mathbf{J}(\mathbf{r}',\tau)}{4\pi R\epsilon}-\frac{\dot{\Pi}(\mathbf{r}',\tau)}{4\pi R}\right]dS'=\dot{\Phi}^{\text{inc}}(\mathbf{r},t), \quad (9)$$

2.2. Discretization

This new D-APIE can be discretized using the separable expansion of the time domain Green's function described in [5]. The approach is to approximate the time domain Green's function using an expansion that separates the Green's function into independent spatial and temporal parts. This is done with the completeness relation for the Legendre polynomials,

$$\sum_{l=0}^{\infty}\frac{2l+1}{2}P_l(x')P_l(x)=\delta(x-x'), \quad (10)$$

which is used to expand the delta function in the Green's function. This greatly simplifies the numerical integrations needed for evaluating matrix elements as the temporal and spatial integrals are now almost independent of each other.

The actual factorization of the Green's function begins as

$$g(\mathbf{r},\mathbf{r}',t)=\frac{1}{4\pi R}\delta(t-\zeta/c)*\delta\left(t-\frac{R-\zeta}{c}\right), \quad (11)$$

where the convolution with $\delta(t-\zeta/c)$ is used to lower the support that the separable expansion is performed over. In particular, ζ is the largest multiple of $c\Delta t$ between a quadrature point on the testing triangle and the source triangle, as illustrated in Fig. 1. By limiting the separable expansion over a smaller support, quicker convergence in the series expansion is achieved.

Now the separable expansion to the second delta function in (11) can be applied, giving

$$g(\mathbf{r},\mathbf{r}',t)\approx\delta(t-\zeta/c)*\sum_{l=0}^{N_h}a_l P_l(b\,t-1)\frac{P_l(\tilde{R})}{4\pi R}, \quad (12)$$

where $\tilde{R} = b(R-\zeta)/c - 1$, $a_l = b(2l+1)/2$, and the sum has been truncated to N_h terms for numerical implementation. In (12), b is chosen to normalize the argument of the Legendre polynomials so that they cover the entire range of -1 to 1 over the integration region. The exact value of b is

$$b = \frac{2}{\nu \Delta t}, \tag{13}$$

where ν is the smallest integer so that a sphere with radius $c\nu\Delta t$ centered at the observation quadrature point will completely enclose the source triangle (see Fig. 1). Numerical experiments suggest that selecting $N_h = 3\nu$ provides acceptable results [5].

This separable expansion may now be used in a marching-on-in-time (MOT) discretization [5]. When correct temporal basis functions are selected this leads to a stable system. A possible temporal basis function, T, that can be used for these equations is a triangle function, i.e.,

$$T(t) = \begin{cases} 1 - \frac{|t|}{\Delta t}, & \text{for } |t| \le \Delta t \\ 0, & \text{elsewhere,} \end{cases} \tag{14}$$

where Δt is the time step used in the discretization. Note that the stability of these systems in practice is highly dependent on the proper selection of temporal basis and testing functions. Only a basis and testing pair of functions that are members of the correct Sobolev spaces (or are discretely equivalent, [6]) will lead to stable systems over a wide range of excitations. The spatial basis function used for $\mathbf{J}$ are Rao-Wilton-Glisson (RWG) functions (denoted as $\mathbf{f}_n$ for the nth edge), which are defined by

$$\mathbf{f}_n(\mathbf{r}) = \begin{cases} \dfrac{1}{2A_n^+}(\mathbf{r} - \mathbf{r}_n^+), & \mathbf{r} \in T_n^+ \\ -\dfrac{1}{2A_n^-}(\mathbf{r} - \mathbf{r}_n^-), & \mathbf{r} \in T_n^-. \end{cases} \tag{15}$$

In (15), $T_n^\pm$ are the triangles that share the nth internal edge of the triangular mesh. Further quantities are $A_n^\pm$, which are the areas of triangles $T_n^\pm$, and $\mathbf{r}_n^\pm$ which are the vector positions of the vertices of $T_n^\pm$ that are not connected to the nth edge of the mesh. For Π, the spatial basis functions used are pulse functions (denoted as h_m for the mth triangle) which are simply a constant over a triangle, selected to be $1/A$ where A is the area of the triangle. The spatial testing functions are RWG functions for (8) and pulse functions for (9).

Using these basis and testing functions in a MOT procedure produces the following matrix system,

$$\begin{aligned} \begin{bmatrix} \mu_r \Delta t\big(\dot{\mathbf{V}}^{(0)} + \dot{\mathbf{K}}^{(0)}\big) & \mathbf{D}^T\mathbf{S}^{(0)} \\ \mathbf{S}^{(0)}\mathbf{D} & -\frac{\epsilon_r}{c_0^2\Delta t}\dot{\mathbf{S}}^{(0)} \end{bmatrix} \begin{Bmatrix} (c_0\Delta t)^{-1}\mathbf{J}^{(i)} \\ \eta_0^{-1}\boldsymbol{\psi}^{(i)} \end{Bmatrix} &= \begin{Bmatrix} \eta_0^{-1}\boldsymbol{\alpha}^{(i)} \\ \frac{\epsilon}{c_0\Delta t}\boldsymbol{\phi}^{(i)} \end{Bmatrix} \\ - \sum_{j=i-j_{max}}^{i-1} \begin{bmatrix} \mu_r \Delta t\big(\dot{\mathbf{V}}^{(i-j)} + \dot{\mathbf{K}}^{(i-j)}\big) & \mathbf{D}^T\mathbf{S}^{(i-j)} \\ \mathbf{S}^{(i-j)}\mathbf{D} & -\frac{\epsilon_r}{c_0^2\Delta t}\dot{\mathbf{S}}^{(i-j)} \end{bmatrix} \begin{Bmatrix} (c_0\Delta t)^{-1}\mathbf{J}^{(j)} \\ \eta_0^{-1}\boldsymbol{\psi}^{(j)} \end{Bmatrix}, \end{aligned} \tag{16}$$

where η_0 is the intrinsic impedance of free space and c_0 is the speed of light in free space.

The different matrix elements are defined as:

$$[\dot{\mathbf{V}}^{(i-j)}]_{mn} = \int_{S_m}\int_{S_n} \sum_{l=0}^{N_h} a_l \dot{\xi}_l^{(i-j)} \mathbf{f}_m(\mathbf{r}) \cdot \mathbf{f}_n(\mathbf{r}') \frac{P_l(\tilde{R})}{4\pi R} dS' dS, \tag{17}$$

$$[\dot{\mathbf{K}}^{(i-j)}]_{mn} = \begin{cases} \dfrac{1}{2}\displaystyle\int_{S_m} \dot{T}\big((i-j)\Delta t\big)\mathbf{f}_m(\mathbf{r}) \cdot \mathbf{f}_n(\mathbf{r}') dS, & \text{for } m = n \\ -\displaystyle\int_{S_m}\int_{S_n} \sum_{l=0}^{N_h} a_l P_l(\tilde{R}) \Big(\mathbf{f}_m(\mathbf{r}) \cdot \hat{n} \times \mathbf{f}_n(\mathbf{r}') \times \boldsymbol{R}\Big) \Big[\dfrac{\dot{\xi}_l^{(i-j)}}{4\pi R^2 c} + \dfrac{\xi_l^{(i-j)}}{4\pi R^3}\Big] dS' dS, & \text{for } m \ne n, \end{cases} \tag{18}$$

$$[\mathbf{S}^{(i-j)}]_{mn} = \int_{T_m}\int_{T_n}\sum_{l=0}^{N_h} a_l \xi_l^{(i-j)} h_m(\mathbf{r}) h_n(\mathbf{r}') \frac{P_l(\tilde{R})}{4\pi R} dS' dS, \tag{19}$$

$$[\dot{\mathbf{S}}^{(i-j)}]_{mn} = \int_{T_m}\int_{T_n}\sum_{l=0}^{N_h} a_l \dot{\xi}_l^{(i-j)} h_m(\mathbf{r}) h_n(\mathbf{r}') \frac{P_l(\tilde{R})}{4\pi R} dS' dS, \tag{20}$$

where the temporal convolutions are contained in

$$\xi_l^{(i-j)} = \int_{-\infty}^{\infty} P_l(b\,t'-1) T\big(\kappa - t'\big) dt' \tag{21}$$

$$\dot{\xi}_l^{(i-j)} = \int_{-\infty}^{\infty} P_l(b\,t'-1) \dot{T}\big(\kappa - t'\big) dt', \tag{22}$$

and $\kappa = (i-j)\Delta t - \zeta/c$. In these equations, S_n is the support covered by the nth RWG function, and T_n is the support of the nth triangle.

The incidence matrix, denoted by $\mathbf{D}$, is used to account for the bookkeeping related to taking the divergence of the RWG functions. The matrix is simple and is given by

$$[\mathbf{D}]_{mn} = \begin{cases} 1, & \text{patch of } h_m \text{ is the positive triangle of } \mathbf{f}_n \\ -1, & \text{patch of } h_m \text{ is the negative triangle of } \mathbf{f}_n \\ 0, & \text{otherwise.} \end{cases} \tag{23}$$

Finally, the excitations may be calculated as

$$\{\boldsymbol{\alpha}^{(i)}\}_m = \int_{S_m} \mathbf{f}_m(\mathbf{r}) \cdot \Big(-\dot{\mathbf{A}}^{\text{inc}}(\mathbf{r}, i\Delta t) + \hat{n} \times \nabla \times \mathbf{A}^{\text{inc}}(\mathbf{r}, i\Delta t) \Big) dS \tag{24}$$

$$\{\boldsymbol{\phi}^{(i)}\}_m = \int_{T_m} h_m(\mathbf{r}) \dot{\Phi}^{\text{inc}}(\mathbf{r}, i\Delta t) dS. \tag{25}$$

3. NUMERICAL RESULTS

In this section, numerical examples are presented to validate the stability and accuracy of the equations derived throughout this work. Further, it is demonstrated that the new **A**-Φ system presented is free from interior resonances.

For all simulations considered, the scatterer is a PEC sphere with a radius of 1 meter. Since the excitation is assumed to come from the far-field, Φ^{inc} can be set to zero [7]. The incident vector potential is a plane wave with temporal shape defined by a modulated Gaussian pulse,

$$\mathbf{F}^{\text{inc}}(\mathbf{r}, t) = \mathbf{F}_0 \exp\left[-\left(\frac{t_r - t_p}{\sqrt{2}\sigma} \right)^2 \right] \cos(2\pi f_0 t_r). \tag{26}$$

In (26), $\mathbf{F}^{\text{inc}}$ should be selected as the appropriate excitation for the TDIE considered, e.g., $\dot{\mathbf{A}}^{\text{inc}}$. The polarization direction and amplitude are set by $\mathbf{F}_0$, and $t_r = t - \mathbf{r}\cdot\hat{\mathbf{k}}/c$, where $\hat{\mathbf{k}}$ sets the propagation direction. The width of the pulse is set by $\sigma = 3/(2\pi f_{\text{bw}})$, where f_{bw} defines the bandwidth of the pulse. Finally, $t_p = 8\sigma$ and f_0 is the center frequency of the pulse. The time step for the simulations is selected to be a fixed oversampling of the Nyquist frequency. This is done by setting $\Delta t = 1/\big(s(f_0 + f_{bw})\big)$, where s is usually set to 10 or 20.

The first numerical example presented demonstrates that the new D-APIE is free from interior resonances. To illustrate this, we simulate a PEC sphere with an incident pulse that has a center frequency of 225 MHz with a bandwidth of 80 MHz. To highlight the presence of interior resonances, Fig. 2 shows the solved coefficients transformed to the frequency domain for one of the unknowns for both the D-APIE of [1] and the formulation of this work. It is seen that there are perturbations of the frequency response at resonant frequencies of the sphere for the formulation of [1], while

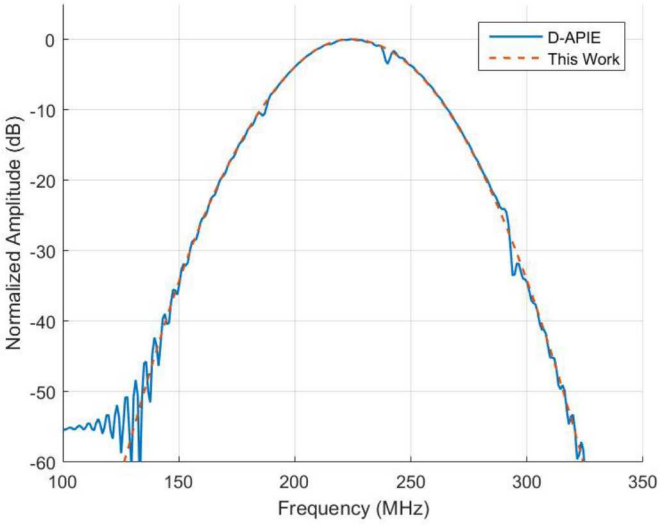

Figure 2: Solved coefficient transformed to the frequency domain for the D-APIE of [1] and the formulation of this work.

the results from this work are smooth. The presence of these perturbations can lead to lower accuracy when extracting parameters of interest, such as the scattering cross section (SCS). More importantly, the interior resonances can lead to instability of the system described in [1], making that method unusable for structures of moderate electrical size.

To demonstrate the accuracy of the new formulation, a sequence of simulations is performed. The SCS is extracted at the center frequency for simulations ranging from 1 Hz to 225 MHz, with the bandwidth set to approximately half the center frequency and s set to 20. The error is calculated by

$$\text{Error} = \frac{||\text{SCS}_{\text{TDIE}} - \text{SCS}_{\text{Mie}}||}{||\text{SCS}_{\text{Mie}}||}, \tag{27}$$

which compares to the analytical Mie series solution for the sphere. The particular results used for computing the error are the E-plane bistatic SCS from 0 to 180 degrees. The results are shown in Fig. 3, which demonstrates that the formulation proposed in this work is able to maintain good accuracy over a very wide range of frequencies. Additionally, it is seen that the error eventually jumps for the D-APIE of [1] due to the interior resonances making the simulations unstable. Note that the slight increase in error for the formulation of this work at higher frequencies is due to the mesh becoming relatively coarse at those frequencies.

4. CONCLUSION

This work presented a new set of $\mathbf{A}$-Φ formulation TDIEs that are not susceptible to interior resonances. This allows the new formulation to be truly multiscale, as one can now maintain good accuracy at both extremely low and high frequencies in contrast to past TDIEs.

Future work will develop an APIE, based on (4) and (5), that is also free from interior resonances. That set of equations performs better at low frequencies than the D-APIE, and also has the benefit of performing the calculation related to $\mathbf{A}$ and Φ directly, as opposed to the temporal derivatives of these quantities. Another important step for this formulation is to develop a set of equations suitable for analyzing dielectric structures. This is necessary for many applications in areas such as quantum optics, where the PEC approximation of materials is no longer applicable.

ACKNOWLEDGMENT

This work was supported by the following sources: Sandia National Laboratories Tuition Assistance Program, AF Sub RRI PO0539, and NSF ECCS 169195.

Sandia National Laboratories is a multimission laboratory managed and operated by National Technology and Engineering Solutions of Sandia LLC, a wholly owned subsidiary of Honeywell

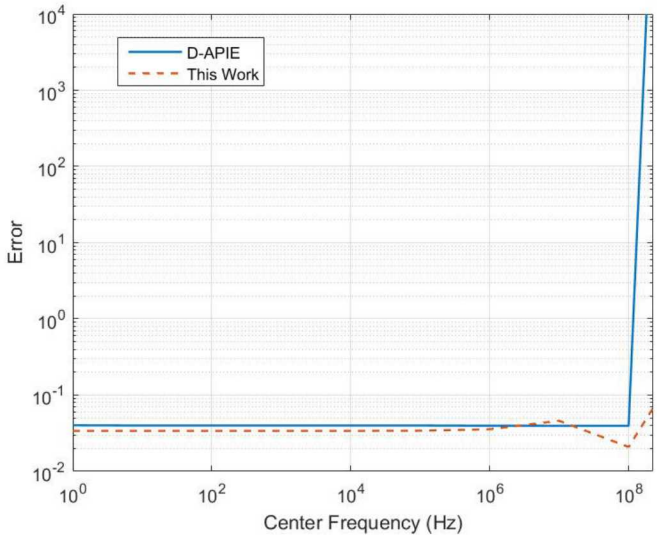

Figure 3: Error over a range of frequencies for the D-APIE of [1] and the formulation of this work.

International Inc., for the U.S. Department of Energy's National Nuclear Security Administration under contract DE-NA0003525.

REFERENCES

1. T. E. Roth and W. C. Chew, "Development of stable A-Φ time domain integral equations for multiscale electromagnetics," under review, 2018.
2. ——, "Stability analysis of A-Φ time domain integral equations for multiscale electromagnetics," in preparation, 2018.
3. B. Shanker, A. A. Ergin, K. Aygun, and E. Michielssen, "Analysis of transient electromagnetic scattering from closed surfaces using a combined field integral equation," *IEEE Transactions on Antennas and Propagation*, vol. 48, no. 7, pp. 1064–1074, 2000.
4. A. Bachelot, L. Bounhoure, and A. Pujols, "Couplage éléments finis-potentiels retardés pour la diffraction électromagnétique par un obstacle hétérogène," *Numerische Mathematik*, vol. 89, no. 2, pp. 257–306, 2001.
5. A. J. Pray, N. V. Nair, and B. Shanker, "Stability properties of the time domain electric field integral equation using a separable approximation for the convolution with the retarded potential," *IEEE Transactions on Antennas and Propagation*, vol. 60, no. 8, pp. 3772–3781, 2012.
6. E. van't Wout, D. R. van der Heul, H. van der Ven, and C. Vuik, "Stability analysis of the marching-on-in-time boundary element method for electromagnetics," *Journal of Computational and Applied Mathematics*, vol. 294, pp. 358–371, 2016.
7. Q. S. Liu, S. Sun, and W. C. Chew, "A potential based integral equation method for low-frequency electromagnetic problems," *IEEE Transactions on Antennas and Propagation*, vol. PP, no. 99, pp. 1–1, 2018.